[12] For recent examples of supramolecular systems deposited on surfaces, see a) P. Laitenberger, C. G. Claissens, L. Kuipers, F. M. Raymo, R. E. Palmer, J. F. Stoddart, *Chem. Phys. Lett.* **1997**, *279*, 209–214; b) G. Ashkenasy, G. Kalyuzhny, J. Libman, I. Rubenstein, A. Shanzer, *Angew. Chem.* **1999**, *111*, 1333–1336; *Angew. Chem. Int. Ed.* **1999**, *38*, 1257–1261; c) M. Lahav, L. Leiserowitz, *Angew. Chem.* **1999**, *111*, 2691–2694; *Angew. Chem. Int. Ed.* **1999**, *38*, 2533–2536; d) A. Semenov, J. P. Spatz, M. Müller, J.-M. Lehn, B. Sell, D. Schubert, C. H. Weidl, U. S. Schubert, *Angew. Chem.* **1999**, *111*, 2701–2705; *Angew. Chem. Int. Ed.* **1999**, *38*, 2547–2550; e) N. Bampos, C. N. Woodburn, M. E. Welland, J. K. M. Sanders, *Angew. Chem.* **1999**, *111*, 2949–2953; *Angew. Chem. Int. Ed.* **1999**, *38*, 2780–2783; f) H. Imahori, H. Yamada, S. Ozawa, K. Ushida, Y. Sakata, *Chem. Commun.* **1999**, 1165–1166; g) D. Ryan, S. N. Rao, H. Rensmo, D. Fitzmaurice, J. A. Preece, S. Wenger, J. F. Stoddart, N. Zaccheroni, *J. Am. Chem. Soc.* **2000**, *122*, 6252–6257; h) M. Lahav, A. N. Shipway, I. Willner, M. B. Nielsen, J. F. Stoddart, *J. Electroanal. Chem.* **2000**, *482*, 217–221; i) G. Cooke, F. M. A. Duclairoir, V. M. Rotello, J. F. Stoddart, *Tetrahedron Lett.* **2000**, *41*, 8163–8166.

[13] C. J. Brinker, G. W. Scherer, *Sol–Gel Science*, Academic Press, San Diego, **1990**.

[14] A silica sol–gel provides a stable transparent matrix for encapsulating molecules physically in a macroscopic solid; see a) B. Dunn, J. I. Zink, *Chem. Mater.* **1997**, *9*, 2280–2291; b) D. Avnir, *Acc. Chem. Res.* **1995**, *28*, 328–334; c) B. Dunn, J. I. Zink, *J. Mater. Chem.* **1991**, *1*, 903–913. The sol–gel process is a synthetic technique for preparing oxide gels, glasses, and inorganic compounds at far lower temperatures than is possible by conventional synthesis. The approach is based on the hydrolysis and condensation of molecular precursors such as metal alkoxides. It has received considerable attention because it possesses a number of desirable characteristics in terms of producing materials of high purity and excellent homegeneity. Moreover, since the sol–gel approach is a solution-based method, it is readily adaptable to producing thin films and fibres as well as bulk materials. The flexible solution chemistry associated with the synthesis of sol–gels makes it possible to incorporate a large variety of organic molecules in the inorganic oxide matrix. The optical properties of the molecular dopants are then imparted upon the solid derived from the sol–gel. Hence this process gives rise to a large number of materials with interesting and unique properties. The interconnected nanopores in sol–gels are filled with liquid which can provide supramolecular machines with a local solution environment in which large molecular movements (co-conformational changes) can be performed, with the silicate framework providing the macroscopic support. The silicate matrix is also transparent to visible light and this transparency makes it possible to study a photoactivated system inside its pores.

[15] This particular BHEEEN derivative with four oxygen atoms present in each of its polyether chains is well suited to maximizing the C–H $\cdots$ O interactions with CBPQT^{4+}; see M. Asakawa, W. Dehaen, G. L'abbé, S. Menzer, J. Nouwen, F. M. Raymo, J. F. Stoddart, D. J. Williams, *J. Org. Chem.* **1996**, *61*, 9591–9595.

[16] a) M. H. Huang, H. M. Soyez, B. Dunn, J. I. Zink, *Chem. Mater.* **2000**, *12*, 231–235; b) F. Nishida, J. McKiernan, B. Dunn, J. I. Zink, C. J. Brinker, A. J. Hurd, *J. Am. Ceram. Soc.* **1995**, *78*, 1640–1648.

[17] I. Haller, *J. Am. Chem. Soc.* **1978**, *100*, 8050–8055.

[18] The derivatization of the silica surface by using monomeric ICPES is important as the first step in the anchoring of the monobenzylated BHEEEN derivative. If this derivative is treated first of all with ICPES prior to silanization, then undesired oligomers are formed on the silica surface.

[19] The derivatized films were immersed in an aqueous solution of CBPQT $\cdot$ 4Cl for two days. The residual percentage (ca. 3.4 %) of unthreaded BHEEEN is shown by T1 in Figure 3b. Dethreading, was effected by immersing the film in an aqueous solution (ca. 4 mL) of NaBH$_4$ (ca. 2 nM) for 2–3 h. The resulting luminescent intensity is shown in D1 in Figure 3b. Threading and dethreading was demonstrated over three redox cycles, namely, T1/D1–T2/D2–T3/D3.

[20] Ordered arrays of molecular motors are essential to the life of a cell; see a) R. A. Cross, *Nature* **2000**, *406*, 839–840; b) T. Hasson, R. E. Cheney, *Curr. Opin. Cell Biol.* **2001**, *13*, 29–35.

[21] P.-L. Anelli, P. R. Ashton, R. Ballardini, V. Balzani, M. Delgado, M. T. Gandolfi, T. T. Goodnow, A. E. Kaifer, D. Philp, M. Pietraszkiewicz, L. Prodi, M. V. Reddington, A. M. Z. Slawin, N. Spencer, J. F. Stoddart, C. Vicent, D. J. Williams, *J. Am. Chem. Soc.* **1992**, *114*, 193–218.

[22] D. B. Amabilino, P.-L. Anelli, P. R. Ashton, G. R. Brown, E. Córdova, L. A. Godinez, W. Hayes, A. E. Kaifer, D. Philp, A. M. Z. Slawin, N. Spencer, J. F. Stoddart, M. S. Tolley, D. J. Williams, *J. Am. Chem. Soc.* **1995**, *117*, 11142–11170.

[23] P. R. Ashton, J. Huff, S. Menzer, I. W. Parsons, J. A. Preece, J. F. Stoddart, M. S. Tolley, A. J. P. White, D. J. Williams, *Chem. Eur. J.* **1996**, *2*, 31–44.

Helical Superstructures of a C_2-Symmetric Molecule Exhibiting Strong Second Harmonic Generation in the Solid-State**

P. Gangopadhyay and T. P. Radhakrishnan*

The design of molecular materials for quadratic nonlinear optical (NLO) applications involves optimization of the structure at both the molecular and the materials level.[1] Molecular design aims at the maximization of the hyperpolarizability (β) as well as the incorporation of structural features that facilitate suitable assembly in the bulk phase. The latter features include hydrogen-bonding functionalities,[2] ionic groups,[3] optimally long alkyl chains,[4] and chirality.[5, 6] Of these, only chirality ensures noncentrosymmetric organization, an essential prerequisite for the observation of quadratic NLO effects. However, even though the basic symmetry requirement is satisfied, efficient exploitation of the inherently strong molecular nonlinear response is rarely achieved at the bulk level. An exceptionally successful case is that of *N*-4-nitrophenyl-(*S*)-prolinol (NPP).[6] We previously investigated the strategic placement of stereogenic centers in push-pull quinonoid molecules to achieve enhanced second harmonic generation (SHG).[7] A logical extension of this study is that an axial chiral system having a strong β component coincident with the symmetry axis would be a promising candidate. We also envisaged that C_2-symmetric molecules could potentially form helical assemblies, the chirality of which extends over the whole molecular superstructure. Recent studies have demonstrated enhanced NLO effects arising from supramolecular chirality in polymers,[8] mesoscopic systems,[9] and Langmuir–Blodgett films.[10] Helical

---

[*] Dr. T. P. Radhakrishnan, P. Gangopadhyay
School of Chemistry
University of Hyderabad
Hyderabad—500046 (India)
Fax: (+91) 40-3012460
E-mail: tprsc@uohyd.ernet.in

[**] Financial support from the DST (Swarnajayanti Fellowship) and the use of the National Single Crystal Diffractometer Facility (funded by the DST at the School of Chemistry, University of Hyderabad) are gratefully acknowledged. P.G. thanks the University Grants Commission for a senior research fellowship. We thank du Pont Deutschland for a generous gift of 1,2-diaminocyclohexane.

Supporting information for this article is available on the WWW under http://www.angewandte.com or from the author.

molecules with large hyperpolarizability have been studied computationally and experimentally.[11] There has been continued interest in the design of helical assemblies of metal complexes[12] and organic molecules.[13] However, to the best of our knowledge, there has been no demonstration of strong SHG in the solid state in structurally characterized organic molecular crystals built up of helical supramolecular assemblies. We have now realized this using the C_2-symmetric *N*,*N*′-bis(4-nitrophenyl)-(1*R*,2*R*)-diaminocyclohexane (BNDC).

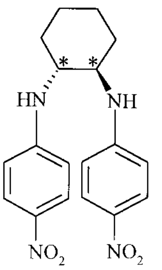

BNDC

There is a brief report of weak SHG observed in the related compound having only one 4-nitrophenyl group,[14] although no structural information is available. We have prepared the bis-substituted product by the reaction of 1,2-diaminocyclohexane with 4-fluoronitrobenzene in the presence of K_2CO_3 in DMSO. Initially we investigated the racemic material, *rac*-BNDC; interestingly it has a noncentrosymmetric crystal structure (Table 1)[15] with molecular tapes generated through intermolecular H-bonds (Figure 1), and exhibits weak SHG in a Kurtz–Perry experiment.[16] The 1*R*,2*R* enantiomer was prepared from carefully isolated, enantiomerically pure (1*R*,2*R*)-diaminocyclohexane. Crystallization of BNDC is found to be very sensitive to the solvent and growth conditions; extensive polymorphism occurs. Crystals grown from ethyl acetate, methanol, and acetone had different platelike morphologies and unit cells. Different batches of crystals from ethyl acetate alone showed two distinct, though very similar, unit cells. Microcrystalline powders of the various crystals showed SHG in the range 5–20 U. We have investigated the crystal structure of thin, long plates of BNDC grown from ethyl acetate (Table 1). They belong to the $P2_12_12_1$ space group, with one molecule in the asymmetric unit. Two types of intermolecular N–H···O interactions lead to the formation of helical assemblies with different pitches that extend along the three crystallographic axes (Figure 2). The helices oriented along the *a* and *b* axes are *M* (left-handed), whereas the one along the *c* axis is *P* (right-handed). Since the orthogonally oriented helices with different handedness do not lead to strong SHG, we explored other solvent systems for crystallization in an effort to produce a lattice structure with helical motifs of a single handedness that are oriented in one direction.

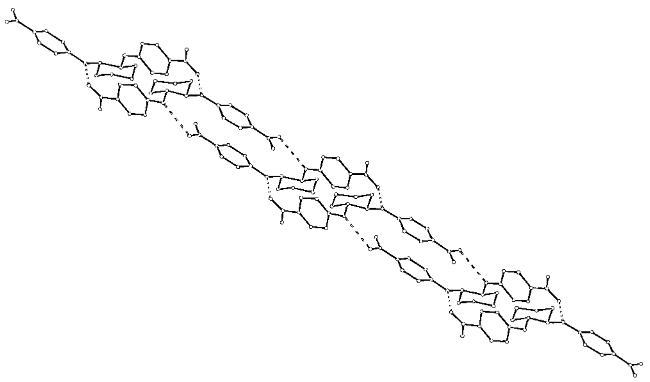

Figure 1. H-bonded tape structure in *rac*-BNDC obtained from a single-crystal X-ray analysis. The alternating molecules are enantiomers. The H-bonds are shown by broken lines.

Crystals with a distinct prismatic morphology different from the earlier cases could be grown from mixtures of ethyl acetate (ea)/hexane and pentan-3-one (diethyl ketone, dek)/hexane. Spectroscopic characterizations indicated the inclusion of solvent molecules, and hence these crystals were labeled as BNDC.ea and BNDC.dek, respectively. Freshly grown crystals show strong SHG (Table 1). However, loss of solvent is observed over a period of a few days leading to opaque crystals or powders with diminished SHG capabilities which melt at 200–204 °C. X-ray investigations showed that both crystals belong to the $C222_1$ space group and have similar cell dimensions (Table 1) and identical lattice structures. The asymmetric unit consists of a half molecule each of BNDC and the solvent; a C_2 operation generates the other halves. The BNDC molecules form *M*-helices that extend solely along the *c* axis, with disordered solvent molecules in the helical channels. Both the nitro and amino groups are involved in noncovalent interactions between the BNDC molecules, thus ruling out any strong interactions with the solvent molecules. Since no weak interactions are found either, we carried out crystallizations from pentan-2,4-dione (acetyl acetone, acac) to take advantage of the possible weak interactions between the solvent molecules and BNDC.

Table 1. Significant crystallographic data and powder SHG capability of the various crystals.[a]

	rac-BNDC	BNDC	BNDC · ea	BNDC · dek	BNDC · acac
formula of asymmetric unit	$C_{36}H_{40}N_8O_8$	$C_{18}H_{20}N_4O_4$	$C_{11}H_{14}N_2O_3$	$C_{11.5}H_{15}N_2O_{2.5}$	$C_{11.5}H_{14}N_2O_3$
space group	$P2_1$	$P2_12_12_1$	$C222_1$	$C222_1$	$C222_1$
a [Å]	10.210(4)	10.2375(19)	11.793(2)	12.084(2)	12.3650(11)
b [Å]	15.34(2)	12.827(2)	15.737(3)	15.847(3)	15.8963(10)
c [Å]	11.933(3)	13.662(9)	12.750(4)	12.935(3)	12.5817(9)
β [°]	109.43(3)	90	90	90	90
V [Å^3]	1762(3)	1794.0(13)	2366.1(10)	2477.0(9)	2473.0(3)
Z	2	4	8	8	8
no. of refl. with	$I \geq \sigma_I$ 3104	$I \geq \sigma_I$ 1813	$I \geq \sigma_I$ 1190	$I \geq 2\sigma_I$ 1287	$I \geq \sigma_I$ 1221
total no. of param.	469	235	156	150	159
$R(I \geq 2\sigma_I)$	0.0453	0.0454	0.0514	0.0689	0.0446
SHG	6 U	20 U	0.93 NPP	1.01 NPP	1.15 NPP

[a] 1 U = SHG of urea with an average particle size ≥ 150 µm, 1 NPP = SHG of NPP with an average particle size ≥ 175 µm (our calibration measurements gave 1 NPP = 115 U; reported values for NPP are in the range 50–150 U.[5, 6, 14]

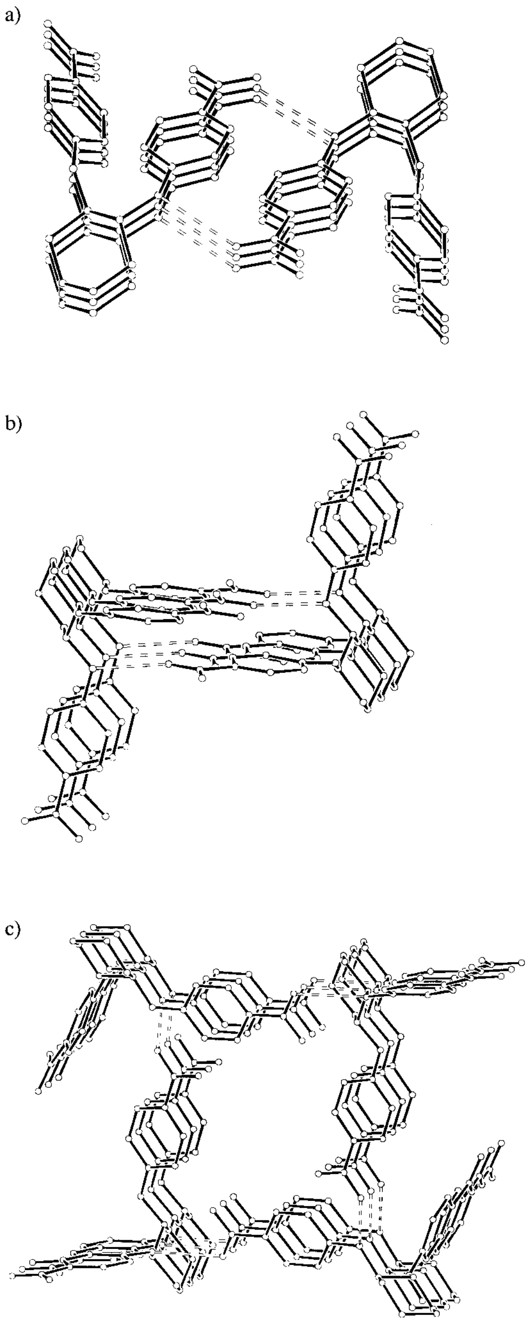

Figure 2. Helical superstructures in BNDC obtained from single-crystal X-ray analysis: view along the helical axis parallel to the *a* (a), *b* (b), and *c* axes (c). The H-bonds are shown by broken lines.

Prismatic crystals were grown by diffusion of hexane into a solution of BNDC in acetyl acetone. The BNDC.acac crystals are found to be considerably more stable than the earlier two toward solvent loss at room temperature; when heated the crystals show a shrinkage at 130–135 °C as a consequence of solvent expulsion, and then melt at 202 °C. Strong SHG, which is stable over several weeks, is observed in the crystals, and a powder study showed a phase-matchable SHG 1.15 times that of NPP (Table 1). An X-ray study once again showed a $C222_1$ space group with cell dimensions and molecular structure similar to BNDC.ea and BNDC.dek, and with an identical lattice structure. The C_2-symmetric BNDC molecules assemble into a beautiful *M*-helix extending along the *c* axis (Figure 3 a, b) and with a dipolar interaction between the nitro groups of neighboring molecules. N–O bonds of adjacent molecules are oriented in an antiparallel

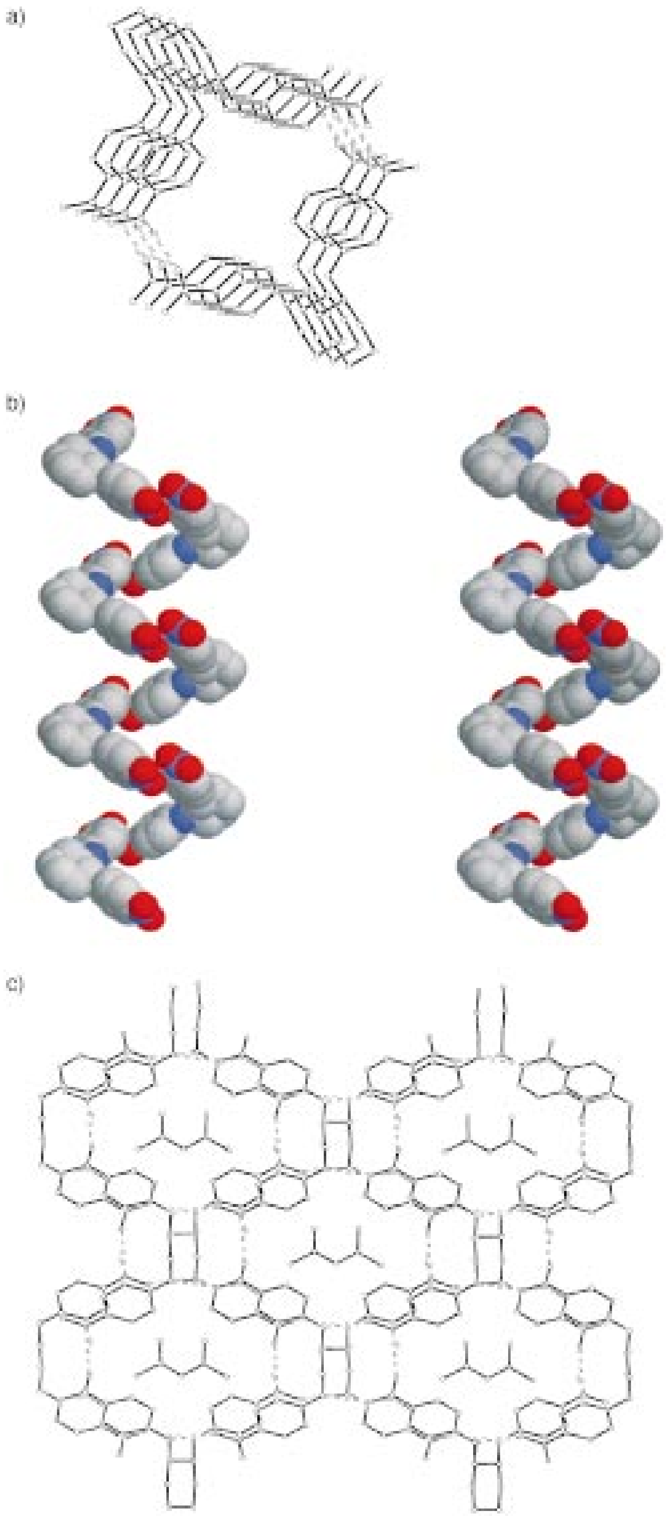

Figure 3. The helical superstructure in BNDC.acac obtained from a single-crystal X-ray analysis: a) view along the helical axis (*c* axis), and b) stereoview perpendicular to the helical axis (space-filling representation). Solvent molecules are omitted for clarity. c) View of the packing of helical channels (projection onto the *ab* plane) including the solvent molecules. The H-bonds and interactions of the nitro groups are shown by broken lines.

manner to form a gently twisted parallelogram with sides of length 1.230 Å (N–O) and 3.175 Å (nonbonded N$\cdots$O), and angles of 105.1° (N-O$\cdots$N) and 73.6° (O-N$\cdots$O). The helical superstructures assemble to form the lattice shown in Figure 3c through formation of intermolecular H-bonds between the amino and nitro groups, with an N$\cdots$O distance of 3.003 Å and an N-H$\cdots$O angle of 143.9°. The two oxygen atoms of the nitro group participate in the dipolar and H-bonding interactions, respectively. The acetyl acetone solvent molecules exist in the helical channels; unlike the earlier two cases, there is no sign of disorder. The central carbon atom lies on the C_2 axis and the bond lengths clearly indicate an enol structure. Several weak H-bonding interactions are observed between the central sp^2 carbon atom of acetyl acetone and the amino nitrogen and the phenyl ring carbon atoms on the BNDC molecule in its vicinity (the shortest C$\cdots$N and C$\cdots$C distances are 3.733 and 3.623 Å, respectively). The oxygen atoms of acetyl acetone also show weak interactions with some of the phenyl ring carbon atoms of BNDC (the shortest C$\cdots$O distances are 3.612 and 3.855 Å). The cooperative effect of these interactions appears to stabilize the solvent molecules in the helical channels.

The asymmetric unit in BNDC·acac (as well as the other two solvated ones) is the half molecule *N*-alkyl-4-nitroaniline. Taking into account its orientation with respect to the crystal axes we have used the oriented gas model[17] to estimate the effective susceptibility coefficient b_{XYZ} (notation of ref. [17]) as 0.151. This value is smaller than the theoretical limit of 0.192 for the 222 point group, but is higher than the value in the well-known NLO crystal 3-methyl-4-nitropyridine-1-oxide (POM)[18] and may be contrasted with the b_{YXX} value of 0.380 in NPP.[6] We have estimated the hyperpolarizability of the half unit of the BNDC molecule at 1.17 eV to be 23.7×10^{-30} esu by using semiempirical AM1/TDHF[19] computation on the full molecule and by assuming a vectorial addition of the contributions of the half units (calculated β tensor components show that the usual 1D model is appropriate for BNDC as well as the half unit). The $\beta_{1.17}$ value of NPP from AM1/TDHF calculations is 29.2×10^{-30} esu; the experimental value[20] is $42 \pm 9 \times 10^{-30}$ esu. In the absence of any information at the moment on the local field factors and phase-matching conditions in BNDC·acac, we assume these factors to be similar to those in NPP. The approximate ratio of the effective susceptibilities of BNDC·acac:NPP then works out to be 0.32:1, which implies a ratio of 0.1:1 between the SHGs of the powders (for details see the Supporting Information). Even if allowance is made for error margins on this estimate, the observed powder SHG of BNDC·acac which is comparable to that of NPP and is very much larger than is suggested by the ratio above. The discrepancy may be traced to one of the following effects in BNDC·acac: the modification of local field factors leading to enhanced bulk susceptibility; an optimal combination of the phase-matching conditions;[16] or the extended helical superstructure giving rise to an enhancement of the β value over that calculated for a single molecule. In view of the basic NLO chromophore being the traditional 4-nitroaniline moiety and the recent demonstrations of enhanced nonlinearity in aggregate structures,[8–10] the helical superstructure appears to be the most probable cause of the enhanced SHG in BNDC·acac. A complete resolution of this question has to await single-crystal SHG measurements for which large enough crystals are not as yet available.

The BNDC crystals illustrate the facile formation of helical supramolecular assemblies from simple building blocks. An examination of the relation between the solvent of crystallization and the superstructures formed is instructive. Crystallization from ethyl acetate resulted in the mutually orthogonal helical motifs assembled solely through the formation of H-bonds. The addition of nonpolar hexane to ethyl acetate led to the realization of dipolar interactions of the nitro group and the single helical motif. Retention of the solvent molecules is critically dependent on their capability to enter into weak noncovalent interactions with the channel walls. These observations provide a basis for further exploration of these helical architectures. The robust channel structure, which accommodates different solvent molecules, suggests the possibility of incorporating a variety of active species in a chiral environment. The strong SHG together with the thermal stability and versatility of the structural framework points to the potential of helical superstructures in the design of efficient molecular NLO materials.

Received: January 15, 2001
Revised: April 5, 2001 [Z16422]

---

[1] a) J. Zyss, D. S. Chemla in *Nonlinear Optical Properties of Organic Molecules and Crystals*, *Vol. 1* (Eds.: D. S. Chemla, J. Zyss), Academic Press, New York, **1989**, p. 23; b) N. J. Long, *Angew. Chem.* **1995**, *107*, 37; *Angew. Chem. Int. Ed. Engl.* **1995**, *34*, 21; c) J. Zyss, J. F. Nicoud, *Curr. Opin. Solid State Mater. Sci.* **1996**, *1*, 533.

[2] a) C. Serbutoviez, J. F. Nicoud, J. Fischer, I. Ledoux, J. Zyss, *Chem. Mater.* **1994**, *6*, 1358; b) K. Huang, D. Britton, M. C. Etter, S. R. Byrn, *J. Mater. Chem.* **1995**, *5*, 379.

[3] S. R. Marder, J. W. Perry, W. P. Schaefer, *Science* **1989**, *245*, 626.

[4] a) P. Gangopadhyay, S. Sharma, A. J. Rao, D. N. Rao, S. Cohen, I. Agranat, T. P. Radhakrishnan, *Chem. Mater.* **1999**, *11*, 466; b) P. Gangopadhyay, T. P. Radhakrishnan, *Chem. Mater.* **2000**, *12*, 3362.

[5] D. F. Eaton, *Science* **1991**, *253*, 281.

[6] J. Zyss, J. F. Nicoud, M. Coquillay, *J. Chem. Phys.* **1984**, *81*, 4160.

[7] M. Ravi, D. N. Rao, S. Cohen, I. Agranat, T. P. Radhakrishnan, *Chem. Mater.* **1997**, *9*, 830.

[8] M. Kauranen, T. Verbiest, C. Boutton, M. N. Teerenstra, K. Clays, A. J. Schouten, R. J. M. Nolte, A. Persoons, *Science* **1995**, *270*, 966.

[9] K. Clays, E. Hendrickx, T. Verbiest, A. Persoons, *Adv. Mater.* **1998**, *10*, 643.

[10] a) T. Verbiest, S. V. Elshocht, M. Kauranen, L. Hellemans, J. Snauwaert, C. Nuckolls, T. J. Katz, A. Persoons, *Science* **1998**, *282*, 913; b) S. V. Elshocht, T. Verbiest, M. Kauranen, L. Ma, H. Cheng, K. Y. Musick, L. Pu, A. Persoons, *Chem. Phys. Lett.* **1999**, *309*, 315.

[11] a) M. Panda, J. Chandrasekhar, *J. Am. Chem. Soc.* **1998**, *120*, 13517; b) H.-J. Deussen, E. Hendrickx, C. Boutton, D. Krog, K. Clays, K. Bechgaard, A. Persoons, T. Bjørnholm, *J. Am. Chem. Soc.* **1996**, *118*, 6841.

[12] a) B. F. Abrahams, S. R. Batten, H. Hamit, B. F. Hoskins, R. Robson, *Chem. Commun.* **1996**, 1313; b) C. Piguet, G. Bernardinelli, G. Hopfgartner, *Chem. Rev.* **1997**, *97*, 2005; c) H. C. Aspinall, J. F. Bickley, J. L. M. Dwyer, N. Greeves, A. Steiner, *Angew. Chem.* **2000**, *112*, 2980; *Angew. Chem. Int. Ed.* **2000**, *39*, 2858.

[13] a) T. B. Norsten, R. McDonald, N. R. Branda, *Chem. Commun.* **1999**, 719; b) J. R. Koe, M. Fujiki, M. Motonaga, H. Nakashima, *Chem. Commun.* **2000**, 389; c) J. H. K. K. Hirschberg, L. Brunsveld, A. Ramzi, J. A. J. M. Vekemans, R. P. Sijbesma, E. W. Meijer, *Nature* **2000**, *407*, 167.

[14] J. F. Nicoud, R. J. Twieg in *Nonlinear Optical Properties of Organic Molecules and Crystals, Vol. 2* (Eds.: D. S. Chemla, J. Zyss), Academic Press, New York, **1989**, p. 221.
[15] Crystallographic data (excluding structure factors) for the structures reported in this paper have been deposited with the Cambridge Crystallographic Data Centre as supplementary publication nos. CCDC-155121 – 155125. Copies of the data can be obtained free of charge on application to CCDC, 12 Union Road, Cambridge CB21EZ, UK (fax: (+44) 1223-336-033; e-mail: deposit@ccdc.cam.ac.uk).
[16] S. K. Kurtz, T. T. Perry, *J. Appl. Phys.* **1968**, *39*, 3798. All the BNDC crystals are transparent yellow; powder SHG measurements were carried out using a nanosecond-pulsed Nd:YAG laser operating at 1064 nm.
[17] J. Zyss, J. L. Oudar, *Phys. Rev. A* **1982**, *26*, 2028.
[18] a) J. Zyss, D. S. Chemla, J. F. Nicoud, *J. Chem. Phys.* **1981**, *74*, 4800; b) M. Sigelle, R. Hierle, *J. Appl. Phys.* **1981**, *52*, 4199.
[19] a) M. J. S. Dewar, E. G. Zoebisch, E. F. Healy, J. J. P. Stewart, *J. Am. Chem. Soc.* **1985**, *107*, 3902; b) M. Dupuis, S. Karna, *J. Comput. Chem.* **1991**, *12*, 487; c) MOPAC93, Fujitsu Inc.
[20] M. Barzoukas, D. Josse, P. Fremaux, J. Zyss, J. F. Nicoud, J. O. Morley, *J. Opt. Soc. Am. B* **1987**, *4*, 977.

A New Family of Layered Molybdenum(V) Cobalto-Phosphates Built up of $[H_{14}(Mo_{16}O_{32})Co_{16}(PO_4)_{24}(H_2O)_{20}]^{10-}$ Wheels

Charlotte du Peloux, Anne Dolbecq, Pierre Mialane, Jérôme Marrot, Eric Rivière, and Francis Sécheresse*

Metal – oxo cluster compounds exhibit unusual topological properties, and are attractive in view of their use in various fields ranging from catalysis to medicine.[1] Self-assembly processes involving Mo^V lead to a structurally diverse family of well-defined ring-shaped nanoparticles or clusters,[2] and it has been shown recently that such compounds can be connected in several different ways to design extended solids.[3] An alternative way to this step-by-step aggregation process for the design of oxomolybdenum frameworks is the one-pot hydrothermal method. Hydrothermal synthesis of fully reduced molybdenum phosphates has thus been extensively used to prepare solid-state materials. The octahedral coordination of the metal centers combined with the tetrahedral geometry of the phosphate groups is at the origin of a large variety of structures, ranging from one-dimensional polymers to three-dimensional open frameworks.[4] Among these materials, to our knowledge, the only examples of molybdenum phosphates that incorporate first-row transition metals are based on the same building unit, namely the well-characterized $[P_4Mo_6O_{25}(OH)_3]^{3-}$ ion.[5] We describe here the synthesis, structure, and magnetic properties of the new two-dimensional cobaltomolybdenum phosphate **1**, which is constructed from unprecedented large structural groups containing sixteen Co^{II} and sixteen Mo^V ions. These groups are linked by four dicobalto bridges. The related compound **2** has been also isolated and characterized by X-ray diffraction. The structure of **2** contains the same basal units connected by four tetrahedral Co^{II} centers.

$$[(Mo_2O_4)_8(HPO_4)_{14}(PO_4)_{10}\{Co_{22}Cl_2(H_2O)_{42}\}]\cdot 28\,H_2O \qquad \mathbf{1}$$

$$[(Mo_2O_4)_8(HPO_4)_{14}(PO_4)_{10}\{Co_{19}Na_4(H_2O)_{34}\}]\cdot 14\,H_2O \qquad \mathbf{2}$$

Reaction of sodium molybdate with Mo metal as reducing agent, phosphoric acid, and Co^{II} chloride under hydrothermal conditions gave, for a starting pH of 2.0, red parallelepiped crystals of **1** in good yield and, for an initial pH of 3.9 and a smaller amount of Co^{II}, dark purple crystals of the related compound **2**. A single-crystal structure determination of **1**[6] revealed a two-dimensional network. The structure can be described as building groups containing sixteen molybdenum centers and four tetramers of cobalt that form a wheel with a diameter of 19 Å with overall C_{4v} symmetry (Figure 1 a). Valence bond summations have been applied on all atoms to confirm the valence of the metal atoms and to locate water molecules and fourteen terminal hydroxo groups of the

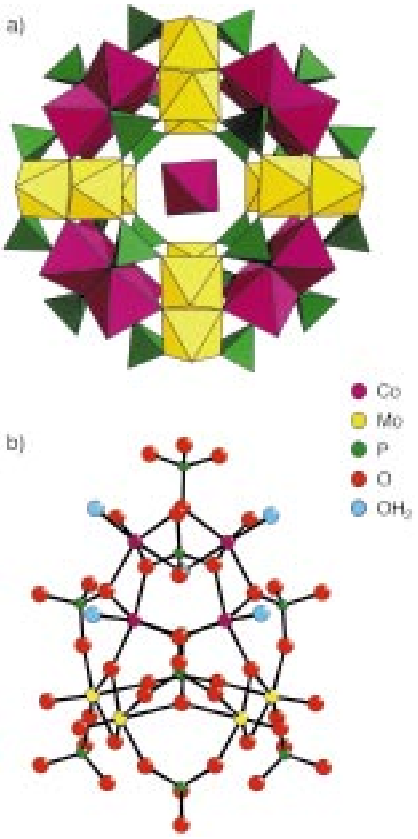

Figure 1. a) Polyhedral representation of the building unit in **1** and **2**; b) ball-and-stick side view of one quarter of the building unit showing the tetramers of Co^{II} and Mo^V.

---

[*] Prof. F. Sécheresse, C. du Peloux, Dr. A. Dolbecq, Dr. P. Mialane, Dr. J. Marrot
Institut Lavoisier, IREM, UMR 8637
Université de Versailles Saint-Quentin
45 Avenue des Etats-Unis, 78035 Versailles (France)
Fax: (+33) 1-39-25-43-81
E-mail: secheres@chimie.uvsq.fr

Dr. E. Rivière
Laboratoire de Chimie Inorganique, URA CNRS 420
Institut de Chimie Moléculaire d'Orsay
Université Paris-Sud
91405 Orsay (France)